



Evolution of karst conduit networks

M. Perne et al.

[Title Page](#)

[Abstract](#)

[Introduction](#)

[Conclusions](#)

[References](#)

[Tables](#)

[Figures](#)



[Back](#)

[Close](#)

[Full Screen / Esc](#)

[Printer-friendly Version](#)

[Interactive Discussion](#)



This discussion paper is/has been under review for the journal Hydrology and Earth System Sciences (HESS). Please refer to the corresponding final paper in HESS if available.

Evolution of karst conduit networks in transition from pressurised flow to free surface flow

M. Perne^{1,2,3}, M. D. Covington³, and F. Gabrovšek¹

¹Karst Research Institute, Research Centre of the Slovenian Academy of Sciences and Arts, Postojna, Slovenia

²Josef Stefan Institute, Ljubljana, Slovenia

³Department of Geosciences, University of Arkansas, Fayetteville, USA

Received: 6 May 2014 – Accepted: 6 June 2014 – Published: 19 June 2014

Correspondence to: F. Gabrovšek (gabrovsek@zrc-sazu.si)

Published by Copernicus Publications on behalf of the European Geosciences Union.

Abstract

We present a novel modelling approach to study the evolution of conduit networks in soluble rocks. Unlike the models presented so far, the model allows a transition from pressurised (pipe) flow to a free surface (open channel) flow in evolving discrete conduit networks. It calculates flow, solute transport and dissolutional enlargement within each time step and steps through time until a stable flow pattern establishes. The flow in each time step is calculated by calling the EPA Storm Water Management Model (EPA SWMM), which efficiently solves the 1-D Saint Venant equations in a network of conduits. We present several cases with low dip and sub-vertical networks to demonstrate mechanisms of flow pathway selection. In low dip models the inputs were randomly distributed to several junctions. The evolution of pathways progresses upstream: initially pathways linking outlets to the closest inputs evolve fastest because the gradient along these pathways is largest. When a pathway efficiently drains the available recharge, the head drop along the pathway attracts flow from the neighbouring upstream junctions and new connecting pathways evolve. The mechanism progresses from the output boundary inwards until all inputs are connected to the stable flow system. In the pressurised phase, each junction is drained by at least one conduit, but only one conduit remains active in the vadose phase. The selection depends on the initial geometry of a junction, initial distribution of diameters, the evolution in a pressurised regime, and on the dip of the conduits, which plays an important role in vadose entrenchment. In high dip networks, the vadose zone propagates downwards and inwards from the rim of the massif. When a network with randomly distributed initial diameters is supplied with concentrated recharge from the adjacent area, the sink point regresses up upstream along junctions connected to the prominent pathways. Large conductive structures provide deep penetration of high hydraulic head and give rise to high gradients and possible fast evolution of conduit systems deep within the massif.

Evolution of karst conduit networks

M. Perne et al.

[Title Page](#)

[Abstract](#)

[Introduction](#)

[Conclusions](#)

[References](#)

[Tables](#)

[Figures](#)

[⏪](#)

[⏩](#)

[◀](#)

[▶](#)

[Back](#)

[Close](#)

[Full Screen / Esc](#)

[Printer-friendly Version](#)

[Interactive Discussion](#)



1 Introduction

Karst aquifers are among the most prolific water reservoirs. Due to their heterogeneity and anisotropy, their efficient exploitation and protection face many challenges. The role of solution conduits in karst aquifers has been a topic of numerous studies. Estimates show that conduits carry about 99 % of flow within karst aquifers and present efficient transport pathways for potential pollutants (Worthington, 1999). However, we have only limited insight into karst aquifers; the position of conduit systems is largely unknown, except for the parts accessible for human exploration or encountered directly by drilling or indirectly by geophysical techniques.

Speleogenesis (e.g. the evolution of conduit networks in karst aquifers) has been one of the main topics in karst studies of the last century. Many conceptual models of speleogenesis have been proposed based on field observations (Audra et al., 2007; Audra and Palmer, 2013; Ford and Ewers, 1978; Palmer, 1991) and inference from basic principles of flow. However, to gain insight into the processes governing speleogenesis, numerical models have been developed based on the physical and chemical principles of flow, dissolution and transport. The main objective of speleogenetic modelling is to determine and evaluate the role of different geological, hydrological and geochemical factors that govern the evolution of conduit networks in karst aquifers.

The modelling of a single conduit (Dreybrodt, 1990, 1996; Palmer, 1991) revealed a feed-back mechanism between flow and dissolution rates and stressed the importance of high order dissolution kinetics (White, 1977; Dreybrodt, 1990, 1996; Palmer, 1991) for the evolution of extended conduits. The initial state of speleogenesis is characterised by slow enlargement of proto-conduits, which is accelerated by positive feedback between flow and dissolution rate. The feedback mechanism ends with *breakthrough*, when flow and widening rate increase by several orders of magnitude in a short time (Dreybrodt and Gabrovsek, 2000).

Individual fractures have been assembled into fracture networks in order to model patterns of evolving conduit systems (Groves and Howard, 1994; Lauritzen et al., 1992;

HESSD

11, 6519–6559, 2014

Evolution of karst conduit networks

M. Perne et al.

Title Page

Abstract

Introduction

Conclusions

References

Tables

Figures

⏪

⏩

⏴

⏵

Back

Close

Full Screen / Esc

Printer-friendly Version

Interactive Discussion



Siemers and Dreybrodt, 1998; Liedl et al., 2003; Kaufmann and Braun, 2000). These models revealed the competition between different pathways connecting inputs to outputs. During the initial phase, the most successful pathway diminishes hydraulic head gradients along the competing pathways, so that they practically cease to grow until the winning pathway breaks through. After the breakthrough of the winning pathway, the field of hydraulic potential changes, and gradients along other pathways build up again. The network integrates to a branchwork or maze pattern, depending on the availability and distribution of recharge (Palmer, 1991, 2007b). Modelling of unconfined networks demonstrated the important role of changing water table in speleogenesis and the formation of base level conduits (Gabrovšek and Dreybrodt, 2001; Kaufmann, 2003). Many other scenarios of early speleogenesis have been modelled to study factors such as the role of geochemical conditions and mixing corrosion, exchange flow between the matrix and conduit network, and the role of insoluble rocks in the evolution of conduits (Dreybrodt et al., 2005). Numerical models have been also used to assess increased leakage at dam sites or other hydraulic structures where unnaturally high hydraulic gradients cause short breakthrough time (Dreybrodt, 1996; Romanov et al., 2003; Hiller et al., 2011).

Modelling of karst network evolution has so far been limited to scenarios with pressurised flow, where many mechanisms of early speleogenesis have been revealed. Nevertheless, in nature one expects that the available recharge cannot sustain pressurised flow within the evolving network, and the conduits undergo a transition from pressurised to free surface flow. Most accessible cave systems have undergone such a transition. To define and explore speleogenetic mechanisms in the latter stages of speleogenesis, a new model is presented here, which accounts for the transition to a free surface flow regime and further evolution in the vadose phase.

In the following sections we describe how the model is built and present two basic modelling scenarios, each with several representative cases. The results are discussed in view of the relevant conceptual models.

HESSD

11, 6519–6559, 2014

Evolution of karst conduit networks

M. Perne et al.

Title Page

Abstract

Introduction

Conclusions

References

Tables

Figures

⏪

⏩

◀

▶

Back

Close

Full Screen / Esc

Printer-friendly Version

Interactive Discussion



2 The model set up

2.1 The conceptual approach

Figure 1 shows a conceptual framework for the modelling presented in this work. We assume a plane populated with conduits with water-soluble walls. Water enters the conduit network at selected junctions indicated by arrows in Fig. 1. The direct recharge into a junction is limited either by the elevation of the land surface (h_{\max}) or by the maximal available recharge Q_{\max} ; if the hydraulic head is lower than h_{\max} , all available recharge (Q_{\max}) enters at the junction, otherwise the hydraulic head at the junction is equal to h_{\max} and only part of the available recharge enters the system.

The basic workflow of the model follows the same scheme as in the models cited above (e.g. Dreybrodt et al., 2005) and includes the following steps:

1. Define the network of conduits and boundary conditions (water inlets and outlets).
2. Calculate flow in the network.
3. Couple flow, dissolution and transport to calculate dissolution rates in all conduits.
4. Change the conduit diameter within a time step according to the dissolution rate and return back to Step 2 or exit the loop when a stable flow pattern is established or no substantial changes in flow pattern are expected.

We also assume that:

1. The flow does not depend on the dissolved load.
2. Time scales for flow, dissolution and transport can be separated from the timescale for widening, i.e. the evolution goes through a set of stationary states within which the widening is constant.

HESD

11, 6519–6559, 2014

Evolution of karst conduit networks

M. Perne et al.

Title Page

Abstract

Introduction

Conclusions

References

Tables

Figures

⏪

⏩

◀

▶

Back

Close

Full Screen / Esc

Printer-friendly Version

Interactive Discussion



2.2 The calculation of flow

We assume that the network has passed the initial (inception) stage of speleogenesis and that turbulent flow has already been established in the network. The reader is referred to work of Dreybrodt et al. (2005) for early evolution in the laminar flow regime.

5 One-dimensional turbulent flow is considered within all conduits. The flow could be either pressurised or free surface.

Flow in partially filled conduits is described by Saint Venant equations (Dingman, 2002), which are based on depth-averaged conservation of mass and momentum. Several numerical techniques are used to solve them (Dingman, 2002). Our model invokes
10 an open source package Storm Water Management Model (abbreviated SWMM from here on), developed primarily for flow and transport simulation in sewage systems by the US Environmental Protection Agency (EPA, 2013). SWMM solves the set of Saint Venant equations to the desired approximation and accuracy using successive approximations with underrelaxation (Rossman, 2009). Its use for the simulation of flow
15 in conduit dominated karst systems has been demonstrated by several authors (e.g. Peterson and Wicks, 2006) The pressurised flow is accounted for by introduction of a fictitious Preissmann slot (Fig. 2) at the top of a conduit's cross-section (Cunge and Wegner, 1964). In this way we transform a pressurised pipe to an open channel without considerably changing the hydraulic characteristics and enable use of the same
20 set of equations for both flow regimes. Friction losses in conduits are calculated by the Manning equation

$$S_f = \frac{n^2 V^2}{R^{4/3}}, \quad (1)$$

where S_f is the friction slope, V the flow velocity, R the hydraulic radius (i.e. the ratio between cross-sectional area of flow and wetted perimeter) and n the Manning roughness coefficient, here taken in the range $0.01 < n < 0.02$.

HESSD

11, 6519–6559, 2014

Evolution of karst conduit networks

M. Perne et al.

Title Page

Abstract

Introduction

Conclusions

References

Tables

Figures

⏪

⏩

◀

▶

Back

Close

Full Screen / Esc

Printer-friendly Version

Interactive Discussion



SWMM enables easy construction of an arbitrary conduit network and many additional elements, such as reservoirs, catchments etc., which could be implemented into future upgrades of the models presented here.

2.3 Dissolution and transport

Dissolution rates in karst environments are determined by the reaction kinetics at the rock-water interface, by diffusion transport of ionic species between the water-rock boundary and the bulk solution, and, in case of limestone, by the rate of CO₂ hydration (Kaufmann and Dreybrodt, 2007). Each of these mechanisms can be rate limiting under certain conditions.

In this work we simplify the dissolution kinetics by assuming a linear rate law at the rock-water boundary:

$$F_s = \alpha_s(c_{\text{eq}} - c_s) \quad (2)$$

α_s is the kinetic constant, c_{eq} is the equilibrium concentration of ionic species of the rock forming mineral and c_s their actual concentration at the surface of the mineral. Ions are transported from the surface into the bulk through a Diffusion Boundary Layer (DBL) of thickness ε (Dreybrodt and Buhmann, 1991). The transport rate through the DBL is given by:

$$F_t = \alpha_t(c_s - c) \quad (3)$$

where α_t is

$$\alpha_t = D/\varepsilon. \quad (4)$$

D is a diffusion coefficient, ε the thickness of the diffusion boundary layer and c the concentration in the bulk solution. Equating Eqs. (2) and (3) gives an equation for c_s and an expression for the effective rates:

$$F = \alpha(c_{\text{eq}} - c); \quad \alpha = \frac{\alpha_t \alpha_s}{\alpha_s + \alpha_t} \quad (5)$$

Title Page

Abstract

Introduction

Conclusions

References

Tables

Figures

◀

▶

◀

▶

Back

Close

Full Screen / Esc

Printer-friendly Version

Interactive Discussion



α_t depends on the thickness, ε , of the DBL, which is related to the thickness, h , of the viscous sub-layer by Schmid's number (Schlichting and Gersten, 2000):

$$\varepsilon = h \cdot Sc^{-1/3}, \quad Sc = \frac{\nu}{D}, \quad (6)$$

5 where ν is kinematic viscosity and Sc the Schmidt number, which represents the relation between the viscous diffusion rate and mass diffusion rate. The thickness of a viscous layer over a flat wall is given by (Incropera and DeWitt, 2002):

$$h = \frac{5\nu}{\sqrt{\tau_\omega/\rho}}, \quad (7)$$

10 where τ_ω is viscous shear stress at the wall and ρ is the water density.

Viscous shear stress is related to the friction slope S_f

$$\tau_\omega = \rho g S_f R, \quad (8)$$

15 where g is Earth's gravitational acceleration. Taking the Manning relation (Eq. 1) for S_f and inserting Eq. (8) into Eq. (7), gives:

$$h = \frac{5\nu R^{1/6}}{nV}. \quad (9)$$

Inserting Eq. (9) into Eq. (6) and further into Eq. (4), we get an expression for ε and for the transport constant α_t :

$$20 \quad \alpha_t = \frac{n \cdot V \cdot D^{2/3} \cdot \nu^{-2/3}}{5R^{1/6}}. \quad (10)$$

Most cases that we present in this work assume that $\alpha_s \gg \alpha_t$, so that $\alpha \approx \alpha_t$. Therefore, the dissolution rates are transport controlled. Usually higher flow rates bring with

Evolution of karst conduit networks

M. Perne et al.

Title Page

Abstract

Introduction

Conclusions

References

Tables

Figures

⏪

⏩

◀

▶

Back

Close

Full Screen / Esc

Printer-friendly Version

Interactive Discussion



them stronger mixing, lower bulk concentrations and higher dissolution rates. In most situations, the rule of thumb will be: the higher the flow, the higher the dissolution rate.

One case in which dissolution rates are almost entirely surface controlled is presented as well.

The ions entering the water increase its saturation state with respect to the mineral forming the walls, and diminish dissolution rates along the flow pathways. The increase of concentration within each conduit is described by a differential equation derived from a mass balance within an infinitesimal segment of conduit:

$$\frac{dc}{dx} = \frac{F(x) \cdot P(x)}{Q}, \quad (11)$$

where $F(x)$ is dissolution rate at coordinate x along a conduit, Q the flow rate and $P(x)$, the conduit's perimeter at x .

Integration of Eq. (11) along a conduit gives the amount of rock dissolved within the conduit. The dissolved load is added to downstream junction of the conduit and is further on treated as a conservative tracer by the pollutant routing code of SWMM.

In most scenarios presented in this work, transport controlled dissolution prevails. Therefore, dissolution rates are dependent on the flow velocity. A case, where the dissolution rates are almost entirely surface controlled, is also presented.

2.4 Dissolutional enlargement

Dissolution rates are rates of dissolutional enlargement v in $[L T^{-1}]$. In pressurised conduits, the cross-section changes uniformly during dissolution (Fig. 3). In a time step Δt , a conduit enlarges by $v\Delta t$, while its centre remains at the initial position. For a conduit with a free surface flow, only the wetted part of the wall is dissolved. Therefore, a transition from tube to canyon-like channel is expected. Although SWMM allows arbitrary channel geometries, the tube shape is used also during the vadose conditions in our model. To this extend an approximation is used, where the bottom of a conduit with a free surface flow incises with the true rate v and its radius increases

Title Page

Abstract

Introduction

Conclusions

References

Tables

Figures

◀

▶

◀

▶

Back

Close

Full Screen / Esc

Printer-friendly Version

Interactive Discussion



with rate $k \cdot v$, where k is the wetted fraction of the conduit perimeter. The centre of the conduit lowers with the rate $(1 - k)v$.

2.5 The model structure

Two basic settings are presented: first a model of a *Low dip* network is presented as conceptually shown in Fig. 1. This scenario is used to interpret the evolution of conduit network in plan view. In a second scenario, a highly inclined *High dip* network is modelled to discuss the vertical organisation of flow pathways or evolution of conduit network in dimension of length and depth (sensu Ford and Ewers, 1978).

Figure 4 introduces a model structure for the Low dip network. Circular conduits with length L and initial diameter D are assembled in an inclined rectangular grid. The orientation of the grid plane is marked geographically, N, E, S and W. All conduits are 10 m long, with initial diameters on the order of a few millimetres. Water enters the system through selected junctions indicated by arrows on Fig. 4a and flows out on the eastern boundary. Figure 4b presents junction geometry: each junction is defined by an invert elevation h_0 , relative to the base level, an inlet offset h_c , which is the elevation of the conduit inlet relative to the invert elevation, and h_{\max} , the maximal depth of water in the junction. If the hydraulic head at a junction is above h_{\max} , the junction surcharges.

Figure 4c shows a side view of the model. The invert elevations increase from E to W, 1 m per junction. The slope of the W-E conduits is therefore 0.1 and N-S oriented conduits are horizontal. The inlet offset defines how much a conduit can incise. To keep conduits from bottoming out as they incise the inlet offsets, h_c , are set to a large value of 100 m. Maximal depth at junctions h_{\max} is 120 m for all, except for the input junctions where h_{\max} is 111 m. There is no storage at the junctions.

Each of the junctions on the E boundary are connected to a large conduit ($D = 5$ m) that drains water to the outfall (see Fig. 4c). The inverts of these junctions are at the base level and so is the inlet of the outfall conduit. The junctions on the E boundary effectively represent a free outflow of the system along that face.

HESSD

11, 6519–6559, 2014

Evolution of karst conduit networks

M. Perne et al.

Title Page

Abstract

Introduction

Conclusions

References

Tables

Figures

⏪

⏩

◀

▶

Back

Close

Full Screen / Esc

Printer-friendly Version

Interactive Discussion



In the High dip model (Fig. 5), the slope of the network (and therefore the conduits) is 0.99 from top to bottom and 0.1 m from left to right. We use expressions vertical for the steep conduits and horizontal for the gradual ones. Water enters on the top side and exits at the seepage face on the right side. Bottom and left boundaries are impermeable. The model is used to discuss the evolution of cave patterns in the vertical dimension sensu Audra and Palmer (2013) or in the dimension of length and depth sensu Ford and Ewers (Ford and Ewers, 1978). In all junctions, gradual (horizontal) conduits are positioned 1 m above the steep (vertical) conduits, which assures preferential flow along the vertical plane in vadose conditions (see Fig. 5b). Flow along the horizontal conduits is active only when the junction is flooded above their inlets. The outflow is realised as in the Low dip case, with large conduits connecting junctions to outfalls on the right boundary.

3 Results and discussion

3.1 Low-dip networks

We start with a simple scenario where all conduits have the same length (10 m), the same initial diameter (0.005 m) and the same inlet offsets. The network dips from W towards the free outflow boundary on the E side with the slope 0.1 m. The model is run for 50 steps of 300 s, in total 15 000 s. The rock used is salt.

Figure 6 presents six snapshots of the network's evolution. Five inputs with $Q_{\max} = 1000 \text{ L s}^{-1}$ are marked by circles and denoted by 1–5 on Fig. 6a. The left column shows flow rates and flow directions. Flow rates are denoted by line thicknesses and flow directions by colour; red represents flow towards N or W and black towards S or E. If the flow is pressurised, the colours are saturated; pale colours denote conduits with free surface flow. The right column represents channel diameters by line thicknesses and growth rates by colours; the warmer the colour the higher the rate of conduit diameter increase. The isolines in the figures represent the total hydraulic heads

Title Page

Abstract

Introduction

Conclusions

References

Tables

Figures

◀

▶

◀

▶

Back

Close

Full Screen / Esc

Printer-friendly Version

Interactive Discussion



with numbers given in meters and a contour interval of 1 m. The heads are directly calculated at the junctions and interpolated by kriging elsewhere. Note that equipotential lines for the junctions on the E border are not given, as the conduit leading to the outfall is at the base level and large enough to keep the water in these junctions always low.

5 Figure 6a shows the initial situation. All inputs are at the maximal hydraulic heads, and only a small part of available recharge enters the network. High gradient drives fast growth of W–E conduits from I1 and I2 (Fig. 6b and c). Also, pathways heading N and S from I1 and I2 evolve in the pressurised flow regime. To the west of I1 and I2, the development is still slow, as the potential field is flattens towards W. On Fig. 6c, the conduits draining I1 and I2 are pressurised and exhibit large flow and widening rates. 10 The gradients from I3 towards the E boundary build up and drive the evolution of pathways from I3 towards the east. When pathways from I1 and I2 are too large to sustain pressurised flow, the hydraulic head in them drops to their topographic height which attracts additional flow from I3. With further time, the evolution progresses upstream. 15 The flow in pathways draining I4 and I5 also increases; it dominantly follows the straight W–E line, although it is also clearly attracted by vadose pathways leading from I3.

Nevertheless, most of the flow from upstream inputs occurs along a direct line of W–E oriented conduits, which evolve most efficiently (Fig. 6c and d). On Fig. 6e, the I3 has become vadose and in a similar manner now attracts flow from I4 and I5. However, 20 the direct line connecting I4 to the boundary takes most of the flow and grows most efficiently. Figure 6f shows the final stable flow configuration. All the inputs drain all available recharge with the direct pathways between the inputs and the E boundary being the only ones that contain active flow.

25 A detailed look at Fig. 6 reveals that at any time, looking at the conduits draining a particular node, the highest flow rates are along W–E conduits, which consequently evolve more efficiently than other conduits. The inlet offsets of W–E conduits incise faster than others and eventually the water level at the junction falls below the lower edges of the other conduits, leaving only the W–E conduits active. This is schematically shown on Fig. 7a, where two outlets from a junction are compared; outlet 1 evolves

HESSD

11, 6519–6559, 2014

Evolution of karst conduit networks

M. Perne et al.

Title Page

Abstract

Introduction

Conclusions

References

Tables

Figures

◀

▶

◀

▶

Back

Close

Full Screen / Esc

Printer-friendly Version

Interactive Discussion



more during the phreatic stage and, therefore, the bottom of the conduit reaches a lower elevation. Consequently, outlet 1 ultimately captures all water during the vadose entrenchment. Several other realisations of this scenario with different recharge rates at the inputs have ended with the same final distribution of active conduits.

At this point a short note is needed on a stable flow configuration. In case of constant recharge the stable flow situation is considered when all junctions are drained by one conduit only, i.e. there are no downstream bifurcations left. This is the case of Fig. 6f. In most of the other presented model runs few outflow bifurcations might still be present on the last presented (which eventually die out if model is ran long enough). We will use term quasi-stable situation in such situations.

The next step towards less idealised scenarios is to assume that the initial inlet offsets of conduits are randomly distributed within the range of 1 m. Figure 8 shows the network when an *quasi-stable* flow pattern has been established, which is now more complex than in the previous case. The general evolution is similar, progressing upstream, but some N and S oriented conduits may have initial inlets low enough to keep the lowest position until the vadose transition occurs and they capture all the flow from a junction. This is schematically illustrated in Fig. 7b. Figure 9 presents the evolution of a network with initial conduit diameters drawn from a uniform distribution with a range of 10^{-4} m to 10^{-2} m. Initial offsets are the same for all nodes.

Generally, the evolution follows the concepts described in Fig. 6. In the pressurised phase, the selection of efficient pathways depends also on the conduit diameters and the W–E conduits are not necessarily the ones with the highest flow rates.

Figure 10 shows the evolution of total discharge from the network over time. Initially, most of the available recharge flows over the surface. First I1 and I2 integrate with full recharge summing $2 \text{ m}^3 \text{ s}^{-1}$. After the gradient for I3 is increased, I3 integrates and the discharge rises to $3 \text{ m}^3 \text{ s}^{-1}$. Then pathways from I4 and I5 start to contribute as these two pathways integrate.

Another selection mechanism becomes active at the transition to a free surface flow, which is shown on Fig. 11, where a few snapshots of the SW part of the network show

HESSD

11, 6519–6559, 2014

Evolution of karst conduit networks

M. Perne et al.

Title Page

Abstract

Introduction

Conclusions

References

Tables

Figures

◀

▶

◀

▶

Back

Close

Full Screen / Esc

Printer-friendly Version

Interactive Discussion



the evolution of several competing pathways evolving from input I5. The junctions of interest are marked by 1 to 3 and enclosed in grey circles at 4800 s. In the pressurised flow regime (4800 s), the N–S oriented conduits, marked by *a*, grow faster than the W–E oriented conduits marked by *b* at all three junctions, because conduits *a* belong to pathways with smaller resistance to flow.

When the flow is pressurised, the flow partitioning between two competing pathways, connecting the same junctions is divided based on the resistance to flow. Note that conduits *b* are parallel to the dip of the network, while conduits *a* are perpendicular to it. The slope of individual conduits and the distribution of slopes along the pathways plays no role. This is not the case in a free surface flow regime, where the slope of the conduit that drains the node is important. When a junction becomes vadose, the flow from initially larger, but flatter conduits can be redistributed to more favourable steeper conduits. This leads to downstream redistribution of flow which can make part of the network inactive or change the flow from pressurised to free surface or vice versa in some of the conduits. The described situation is schematically shown on Fig. 12, where two pathways, *a* and *b* connect two nodes. Pathway *a* is initially larger, drains more flow, and widens more efficiently in the pressurised phase. When the conduit turns vadose, the flow rates in *a* drop due to the low slope of the channel as it leaves the junction. If, at the transition to free surface flow, the water level in the upstream node has not dropped below the inlet of pathway *b*, the steeper entry into pathway *b* as it leaves the junction causes *b* to incise faster and progressively capture more flow.

Figure 13 presents an quasi-stable flow and network pattern for the case identical to the one presented in Fig. 10, but where the plane of the network is additionally tilted from N to S for 0.3 m per node. The tilting makes flow towards S preferential to flow towards N, which is clearly seen in the resulting pattern. The input I4 now joins I3. Because it is near the boundary, the input I5 has no option to develop towards S, except that the pathway heading S from the input (conduit *a* at I5 in Fig. 12) now persists much longer.

HESSD

11, 6519–6559, 2014

Evolution of karst conduit networks

M. Perne et al.

Title Page

Abstract

Introduction

Conclusions

References

Tables

Figures

⏪

⏩

◀

▶

Back

Close

Full Screen / Esc

Printer-friendly Version

Interactive Discussion



Other scenarios with more complex settings, such as networks with 50×50 nodes and networks with irregular recharge, were modelled and additionally confirmed the observations given above.

Finally we turn to a network where dissolution rate is dominantly surface controlled, as is supposed to be the case for limestone. To this end we have modelled a network, identical to the one presented in Fig. 9, but with α_s , c_{eq} and D set so that dissolution rates are several orders of magnitude smaller and almost entirely depend on the saturation state of the solution rather than flow velocity. Since the system is in the post-inception stage the ratio of discharge to flow length (Q/L) in many flow pathways is high enough that they evolve with the maximal growth rates. All conduits and channels along these pathways incise with the same rate. Figure 14 shows the situation at 500 y, when a quasi-stable flow pattern has evolved and the complete network is vadose. All active channels with flow have almost the same inlet offsets and the same incision rates. Note that growth rates are only apparently larger in smaller channels, because of larger hydraulic diameter; see discussion in Sect. 2.4. The resulting flow pattern is, aside from the initial distribution of diameters and boundary conditions, a consequence of two rules: (1) at each node, channels with high dip drain more flow than horizontal channels, (2) if only horizontal channels drain the node, flow is distributed evenly. The presented scenario is highly idealistic and the results and interpretation should be taken with care. One can hardly envisage such a scenario in nature; the dissolution rates change with changing lithology, the initial offsets are not even, the role of sediments is ignored here, and we may question if purely surface controlled rates are reasonable. However, the model supports the ideas of Palmer (Palmer, 1991), that maze caves develop in situations where Q/L is large along many alternative routes.

3.2 High-dip network

We now turn to the situation where the network is steep (almost vertical). As this networks present vertical cross-section of karst, we omit the geographical notation and use top, bottom, left and right for the sides of the networks.

[Title Page](#)

[Abstract](#)

[Introduction](#)

[Conclusions](#)

[References](#)

[Tables](#)

[Figures](#)

[⏪](#)

[⏩](#)

[⏴](#)

[⏵](#)

[Back](#)

[Close](#)

[Full Screen / Esc](#)

[Printer-friendly Version](#)

[Interactive Discussion](#)



Similar models for laminar flow have been presented by Gabrovsek and Dreybrodt (2001) and by Kaufmann (2003). The basic result of these prior models was a continuous drop of the water table due to increased transmissivity of the network and the formation of base level conduits. If a fixed head boundary was applied, competition between a high conductivity zone along the water table and prominent conduits within the phreatic part of the network resulted in a complex pattern of evolved conduits. For many more scenarios of this modelling approach the reader is referred to the book of Dreybrodt et al. (2005).

3.2.1 Homogenous case with recharge distributed over top nodes

Figure 15 presents a case where all conduits are 10 m long with initial diameter of 0.005 m. A maximum possible recharge of 5 L s^{-1} is distributed to all input nodes (blue arrows on Fig. 15a) on the top. The left column shows flow rates as line thicknesses and colours, as denoted in the legend, at five different time steps. Although the term “*water table*” might not be applicable for such discrete networks, we will use it for the line along the highest flooded nodes (dotted blue lines in Fig. 15c and d). The right column shows the conduit diameters as coded in the colour bar for each figure. Isolines in the left column show the distribution of hydraulic head given in meters.

Initially (Fig. 15a), a small part of the available recharge enters the network. At the top-right all the recharge is drained directly into the outfall junction (marked by a red circle on Fig. 15a). The flow rates within the conduits are small and dominant along the vertical conduits (top to bottom). Flow along horizontal conduits is small and increases from left to right.

After 600 s (Fig. 15b) the entire network is still pressurised. Horizontal conduits have evolved sufficiently to drain more flow brought in by initially developed vertical conduits. Accordingly, the potential gradient becomes oriented to the right and is highest close to the boundary. Conduits at the top-right corner experience fastest growth and capture almost all recharge from the inputs. The flow in the right part of the network is small and the hydraulic potential field is relatively flat there. After 1200 s (Fig. 15c) the top-right

Title Page

Abstract

Introduction

Conclusions

References

Tables

Figures

⏪

⏩

◀

▶

Back

Close

Full Screen / Esc

Printer-friendly Version

Interactive Discussion



corner has become vadose). In this area, the recharge is carried vertically to the water table. The flow rates are highest along the water table and diminish with a distance from it.

However, widening is substantial also below the water table which additional increases the network permeability and downwards retreat of WT. The process continues until the WT drops to the base level and only vertical recharge conduits and a master conduit at the base continue to grow. The vertical conduits have been widened through the entire evolution, the northernmost for the longest time and they are therefore largest. The diameters decrease from top to bottom. On the other hand, the diameter of horizontal channels increase from left to right, as they evolve only below the water table. Therefore, deeper (more southern) conduits have more time to evolve.

3.2.2 Inhomogeneous case

In the case shown on Fig. 16 we assign a more complex distribution of initial conduit diameters. The initial diameter (d_o) of each conduit is constructed as a sum of a group contribution (d_g) which is given to all conduits aligned along the same line, and an individual contribution (d_i). These are both random, sampled from a uniform distribution, where $d_g \in [0, 0.005 \text{ m}]$ and $d_i \in [0, 0.01 \text{ m}]$. The probability that conduits along a certain line get the individual contributions is 0.5. By group contribution, we stress the potential importance of conductive structural lines.

Initial diameter of the top (N) horizontal line of conduits is 0.1 m.

The recharge of 100 L s^{-1} is introduced to the top-left junction (see the blue arrow on Fig. 16a). The two given legends for flow rates and diameters are valid for all figures. At 3000 s (Fig. 16a), about one fourth of the available recharge is captured and drained directly to the outfall by the top line of horizontal conduits.

Pathways along the conduits with initially larger diameters evolve efficiently and capture an increasing amount of flow.

At 9000 s (Fig. 16b) about 70 % of the flow is captured by the junction marked by a blue triangle and denoted by 1 in Fig. 16b. It feeds a line of vertical conduit that

Title Page

Abstract

Introduction

Conclusions

References

Tables

Figures

⏪

⏩

◀

▶

Back

Close

Full Screen / Esc

Printer-friendly Version

Interactive Discussion



discharge into outflows through horizontal conduits. Numbers on the conduits in the top-right region denote flow along the conduits in $L s^{-1}$. The discharge to the outflow diminishes downwards. However, these conduits widen effectively and cannot sustain pressurised regime, so that the position of highest outflow migrates downwards.

By 24 000 s, the outflow position has retreated to the bottom (Fig. 16c). When the vertical pathway downwards from point 1 becomes vadose, it provides a free outflow boundary and triggers the development of pathways draining sink points 2 and 3 (Fig. 16b and c) which soon capture all the flow. On Fig. 16c, the flow along the top line has retreated to point 3 and throughout the remainder of the simulation continues to retreat towards the left to points 4 and 5 (Fig. 16d). Ultimately, the flow is captured by the node at point 5 (Fig. 16e). Similarly, the flow migrates from top to bottom, towards the deeper connecting pathways. Figure 16e shows the stable flow situation at 75 000 s, where all the flow follows one single pathway. Downward and leftward progress is slow is slow because some of the conduits to the left are initially small and the permeability is low. In comparison with a uniform network with distributed recharge, the development follows initially prominent pathways, with progressive upstream flow capturing. Soon after a pathway becomes vadose, the flow is overtaken by the evolving pathways to its west.

3.2.3 The role of prominent structures

The progression mechanism described above, is demonstrated clearly by a final idealised, but telling, example. We assume three vertical conduits (“wells”) with an initial diameter of 0.2 m, extending completely through the domain in the vertical direction.

These are connected with 5 evenly spaced horizontal conduits with initial diameter 0.005 m extending across the domain. All other conduits are effectively impermeable, with a diameter of 10^{-5} m. A maximum possible recharge of $100 L s^{-1}$ is available to the prominent vertical conduits (wells) as marked by the arrows at the top of Fig. 16a.

Initially (Fig. 17a), all conduits are pressurised. There is almost no gradient left of W3, where evolution is slow or none. High gradients exist between W3 and the outfalls,

Title Page

Abstract

Introduction

Conclusions

References

Tables

Figures



Back

Close

Full Screen / Esc

Printer-friendly Version

Interactive Discussion



the highest being along the deepest horizontal conduit, which has the highest flow and evolves most efficiently. As W3 becomes vadose, it presents a free outflow boundary for the flow from its right and the gradient along the horizontal conduits connecting W2 to W3 builds up. These conduits now experience fast evolution with rates increasing from the top to the bottom (Fig. 17b). The mechanism progresses westwards: when W2 becomes vadose, W1 connects to it as shown in Fig. 17c. In Fig. 17d, a stable flow condition is shown, where all the flow follows the wells to the base conduits, which drain the water from the system. The numbers on the right picture of Fig. 18d denote diameters in m.

4 Discussion and conclusion

The models presented here have several limitations that have to be considered, before firm conclusions for the natural scenarios can be made. The model does not account for the evolution of fractures/conduits which are still in a proto state. All evolving conduits are initially turbulent. In all cases, except for one, the dissolution is entirely transport controlled and the dissolution rates locally depend also on the flow velocity, which intuitively makes sense, but raises some questions. When limestone dissolution kinetics are used, the network evolves nearly uniformly.

Nevertheless, the results support several mechanisms proposed previously in conceptual models and suggest several novel mechanisms that one could expect in nature.

Sensu Palmer (1991, 2007) this paper considers the hydrological control of cave patterns, particularly those leading to branchwork cave systems. It clearly demonstrates some of the mechanisms postulated by Palmer (2007b). The most common hydraulic mechanism leading to the branchwork cave pattern is as follows: when a passage effectively drains all available recharge from the surface, the hydraulic head along it drops as it enlarges. This initially occurs in the pressurised flow regime and latter in the open surface flow regime, when the pressure head becomes practically zero and the total head becomes the elevation of the water surface inside the channel. In both cases

[Title Page](#)

[Abstract](#)

[Introduction](#)

[Conclusions](#)

[References](#)

[Tables](#)

[Figures](#)

[⏪](#)

[⏩](#)

[◀](#)

[▶](#)

[Back](#)

[Close](#)

[Full Screen / Esc](#)

[Printer-friendly Version](#)

[Interactive Discussion](#)



the water is drawn towards the passage from the neighbouring pressurised tubes, so that these become tributaries. This mechanism was evident in the low dip and high dip scenario, particularly in inhomogeneous settings.

The *Low dip* model illustrates other important factors that also influence the stable flow pattern. Before the stable configuration is established, there is a competition for flow between conduits draining the same junction. In the pressurised phase, all nodes drain according to their resistance and the distribution of hydraulic heads. The inlet offsets (the vertical positions of conduits within a junction) are lowered with different incision rates. As a junction becomes vadose, the conduit at the lowest position within a junction has an advantage and is a candidate to take all the flow. However, under vadose conditions the conduit's alignment with respect to the dip of the network is also important. Because of the steeper gradient, conduits aligned with the dip carry more flow from the node than conduits perpendicular to the dip and evolve faster.

A combination of all three factors determines which conduit finally drains a node.

Once the stable flow pattern is established, the flow follows a system of conduits that all occupy the lowest position in their upstream junctions. Additionally, the water level within these active conduits is below the inlets of all other conduits that could potentially drain the junctions.

In a homogenous *High dip* scenario, the evolution is focused at the transitional area between pressurised and free surface flow, the "water table". The flow from the surface follows the dip along the vadose channels and then follows conduits close to the water table. The retreat of the phreatic zone ends when the base level conduit is directly fed by the vadose conduits. The end result is a relatively uniformly widened network.

In the inhomogeneous case with a point recharge, a backwards and downward migration of vadose flow as described by Palmer (2007a, p. 265) is observed. Point recharge at the NW side initially follows the N face until the network evolves enough to capture the flow, the sinking point regresses from E to W. In the case of an inhomogeneous network the retreat is not continuous, as the flow is more likely to be captured by conduits coupled to prominent pathways.

Evolution of karst conduit networks

M. Perne et al.

Title Page

Abstract

Introduction

Conclusions

References

Tables

Figures

⏪

⏩

⏴

⏵

Back

Close

Full Screen / Esc

Printer-friendly Version

Interactive Discussion



Deep conductive structures can play important role as they transfer high hydraulic heads deep into the massive and redistribute hydraulic gradients. This way fast evolution along other deep structures can be triggered.

Although the structure, lithology, geochemistry and boundary conditions are much more complex in reality, the basic principles captured in these simple models present building blocks that help us to understand more complex systems. These principles can be in turn verified by careful and thoughtful field observations. Modelling of the later speleogenetic stages should also consider the role of mechanical erosion and sediment transport, which have not been considered here but are part of an ongoing study.

The Supplement related to this article is available online at doi:10.5194/hessd-11-6519-2014-supplement.

Acknowledgements. This work would not have been possible without the support of Slovenian Research Agency, who funded the doctoral work of MP. The work of FG was funded by the project J2-4093. MC and MP were also supported by the National Science Foundation under Grant No. 1226903.

References

- Audra, P. and Palmer, A. N.: 6.17 The vertical dimension of karst: controls of vertical cave pattern, in: Treatise on Geomorphology, edited by: Shroder, J. F., Academic Press, San Diego, 186–206, 2013.
- Audra, P., Bini, A., Gabrovsek, F., Hauselmann, P., Hoglea, F., Jeannin, P., Kunaver, J., Monbaron, M., Sustersic, F., Tognini, P., Trimmel, H., and Wildberger, A.: Cave and karst evolution in the Alps and their relation to paleoclimate and paleotopography, Acta Carsologica, 36, 53–67, 2007.
- Cunge, J. A. and Wegner, M.: Numerical integration of Barré de Saint-Venant's flow equations by means of an implicit scheme of finite differences, La Houille Blanche, 1, 33–39, 1964.

Title Page

Abstract

Introduction

Conclusions

References

Tables

Figures



Back

Close

Full Screen / Esc

Printer-friendly Version

Interactive Discussion



Evolution of karst conduit networks

M. Perne et al.

[Title Page](#)[Abstract](#)[Introduction](#)[Conclusions](#)[References](#)[Tables](#)[Figures](#)[I◀](#)[▶I](#)[◀](#)[▶](#)[Back](#)[Close](#)[Full Screen / Esc](#)[Printer-friendly Version](#)[Interactive Discussion](#)

- Dingman, S. L.: Physical Hydrology, Prentice Hall, Upper Saddle River, NJ, 646 pp., 2002.
- Dreybrodt, W.: The role of dissolution kinetics in the development of karst aquifers in limestone – a model simulation of karst evolution, *J. Geol.*, 98, 639–655, 1990.
- Dreybrodt, W.: Principles of early development of karst conduits under natural and man-made conditions revealed by mathematical analysis of numerical models, *Water Resour. Res.*, 32, 2923–2935, 1996.
- Dreybrodt, W. and Buhmann, D.: A mass-transfer model for dissolution and precipitation of calcite from solutions in turbulent motion, *Chem. Geol.*, 90, 107–122, 1991.
- Dreybrodt, W. and Gabrovsek, F.: Dynamics of the evolution of a single karst conduit, in: *Speleogenesis: Evolution of Karst Aquifers*, edited by: Klimchouk, A., Ford, D. C., Palmer, A., and Dreybrodt, W., National Speleological Society, Huntsville, AL, 184–193, 2000.
- Dreybrodt, W., Gabrovsek, F., and Romanov, D.: Processes of speleogenesis: a modeling approach, in: *Carsologica*, edited by: Gabrovsek, F. and Založba, ZRC, Ljubljana, 375 pp., 2005.
- Ford, D. C. and Ewers, R.: The development of limestone caves in the dimensions of length and depth, *Can. J. Earth Sci.*, 15, 1783–1798, 1978.
- Gabrovšek, F. and Dreybrodt, W.: A model of the early evolution of karst aquifers in limestone in the dimensions of length and depth, *J. Hydrol.*, 240, 206–224, 2001.
- Groves, C. G. and Howard, A. D.: Early development of karst systems. 1. Preferential flow path enlargement under laminar-flow, *Water Resour. Res.*, 30, 2837–2846, 1994.
- Hiller, T., Kaufmann, G., and Romanov, D.: Karstification beneath dam-sites: from conceptual models to realistic scenarios, *J. Hydrol.*, 398, 202–211, doi:10.1016/j.jhydrol.2010.12.014, 2011.
- Incropera, F. P. and DeWitt, D. P.: *Fundamentals of Heat and Mass Transfer*, J. Wiley, New York, 981 pp., 2002.
- Kaufmann, G.: Modelling unsaturated flow in an evolving karst aquifer, *J. Hydrol.*, 276, 53–70, 2003.
- Kaufmann, G. and Braun, J.: Karst aquifer evolution in fractured, porous rocks, *Water Resour. Res.*, 36, 1381–1391, 2000.
- Kaufmann, G. and Dreybrodt, W.: Calcite dissolution kinetics in the system $\text{CaCO}_3\text{-H}_2\text{O-CaCO}_3$ at high undersaturation, *Geochim. Cosmochim. Ac.*, 71, 1398–1410, 2007.

Evolution of karst conduit networks

M. Perne et al.

Title Page

Abstract

Introduction

Conclusions

References

Tables

Figures

⏪

⏩

◀

▶

Back

Close

Full Screen / Esc

Printer-friendly Version

Interactive Discussion



- Lauritzen, S.-E., Odling, N., and Petersen, J.: Modelling the evolution of channel network in carbonate rocks, ISRM Symposium: Eurock '92, 57–62, Chester, UK, 14–17 September, 1992.
- Liedl, R., Sauter, M., Huckinghaus, D., Clemens, T., and Teutsch, G.: Simulation of the development of karst aquifers using a coupled continuum pipe flow model, *Water Resour. Res.*, 39, 1057, doi:10.1029/2001WR001206, 2003.
- Palmer, A. N.: Origin and morphology of limestone caves, *Geol. Soc. Am. Bull.*, 103, 1–21, 1991.
- Palmer, A. N.: *Cave Geology*, Cave Books, Dayton, Ohio, vi, 454 pp., 2007.
- Peterson, E. and Wicks, C.: Assessing the importance of conduit geometry and physical parameters in karst systems using the storm water management model (SWMM), *J. Hydrol.*, 329, 294–305, 2006.
- Romanov, D., Gabrovsek, F., and Dreybrodt, W.: Dam sites in soluble rocks: a model of increasing leakage by dissolutional widening of fractures beneath a dam, *Eng. Geol.*, 70, 17–35, 2003.
- Rossman, L. A.: *Storm Water Management Model, User's Manual, Version 5.0*, US Environmental Protection Agency, Cincinnati, 266 pp., 2009.
- Schlichting, H. and Gersten, K.: *Boundary-Layer Theory*, 8th Edn., Springer, Berlin, Heidelberg, 802 pp., 2000.
- Siemers, J. and Dreybrodt, W.: Early development of karst aquifers on percolation networks of fractures in limestone, *Water Resour. Res.*, 34, 409–419, 1998.
- Storm Water Management Model (SWMM): available at: <http://www.epa.gov/nrmrl/wswrd/wq/models/swmm/> (last access: 17 June 2014), 2013.
- White, W. B.: The role of solution kinetics in the development of karst aquifers, *Mem. Int. Assoc. Hydrogeol.*, 12, 503–517, 1977.
- Worthington, S.: A comprehensive strategy for understanding flow in carbonate aquifers, in: *Karst Modeling: Special Publication 5*, edited by: Palmer, A., Palmer, M., and Sasovsky, I., The Karst Waters Institute, Charles Town, West Virginia, 30–37, 1999.

Evolution of karst conduit networks

M. Perne et al.

Title Page

Abstract

Introduction

Conclusions

References

Tables

Figures

I◀

▶I

◀

▶

Back

Close

Full Screen / Esc

Printer-friendly Version

Interactive Discussion

**Table 1.** List of rate constants and other parameters used in this work.

| Parameter | Notation | Value | Units |
|-------------------------------------|-----------------|---|----------------------------|
| Diffusion coefficient | D | 1.5×10^{-9} salt 1×10^{-9} limestone | $\text{m}^2 \text{s}^{-1}$ |
| Manning roughness coefficient | n | 0.01 or 0.015 | 1 |
| Surface rate constant | α | 1 salt 2×10^{-7} limestone | m s^{-1} |
| Volume Equilibrium concentration | c_{eq} | 0.166 salt 1.1×10^{-4} limestone | 1 |
| Gravitational acceleration, Density | g, ρ | 9.81 | m s^{-2} |
| Density of water | ρ | 10^3 | kg m^{-3} |
| Dynamic Viscosity of water | μ | 10^{-3} | Pa s |

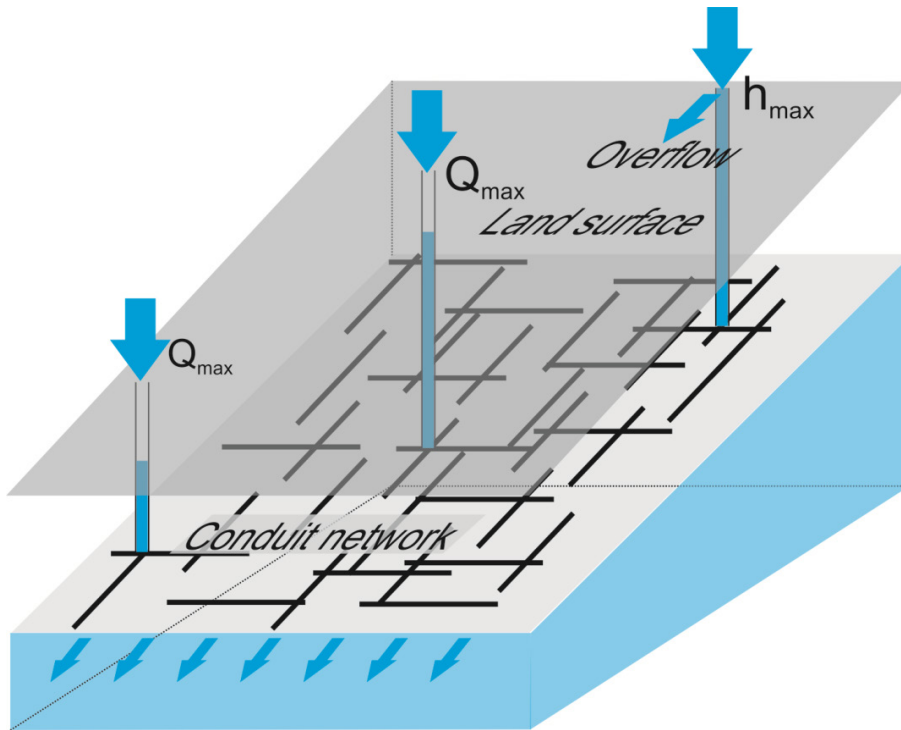


Figure 1. Conceptual framework. A conduit network with point recharge at selected locations (indicated by arrows). Recharge is limited by the position of the land surface h_{\max} or by maximal available recharge Q_{\max} .

HESSD

11, 6519–6559, 2014

Evolution of karst conduit networks

M. Perne et al.

| | |
|--------------------------|--------------|
| Title Page | |
| Abstract | Introduction |
| Conclusions | References |
| Tables | Figures |
| ◀ | ▶ |
| ◀ | ▶ |
| Back | Close |
| Full Screen / Esc | |
| Printer-friendly Version | |
| Interactive Discussion | |



Evolution of karst conduit networks

M. Perne et al.

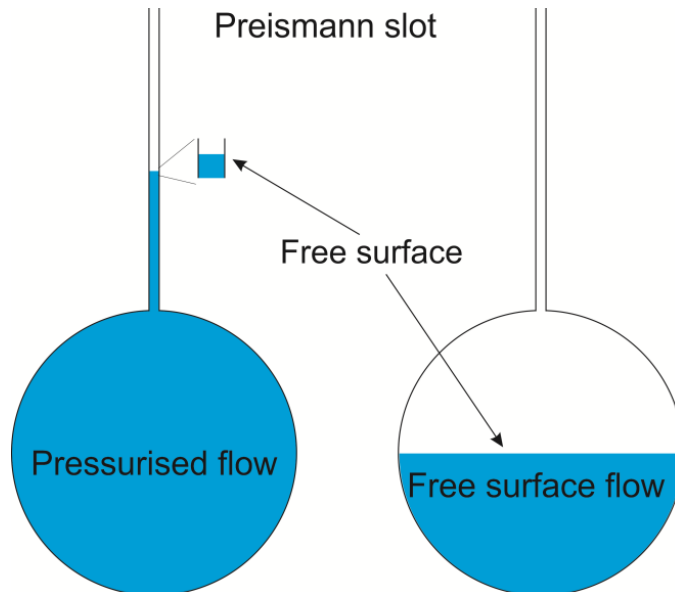


Figure 2. The use of a Preissmann slot enables use of the same set of equations for conduits with free surface flow and conduits with pressurised flow.

[Title Page](#)[Abstract](#)[Introduction](#)[Conclusions](#)[References](#)[Tables](#)[Figures](#)[◀](#)[▶](#)[◀](#)[▶](#)[Back](#)[Close](#)[Full Screen / Esc](#)[Printer-friendly Version](#)[Interactive Discussion](#)

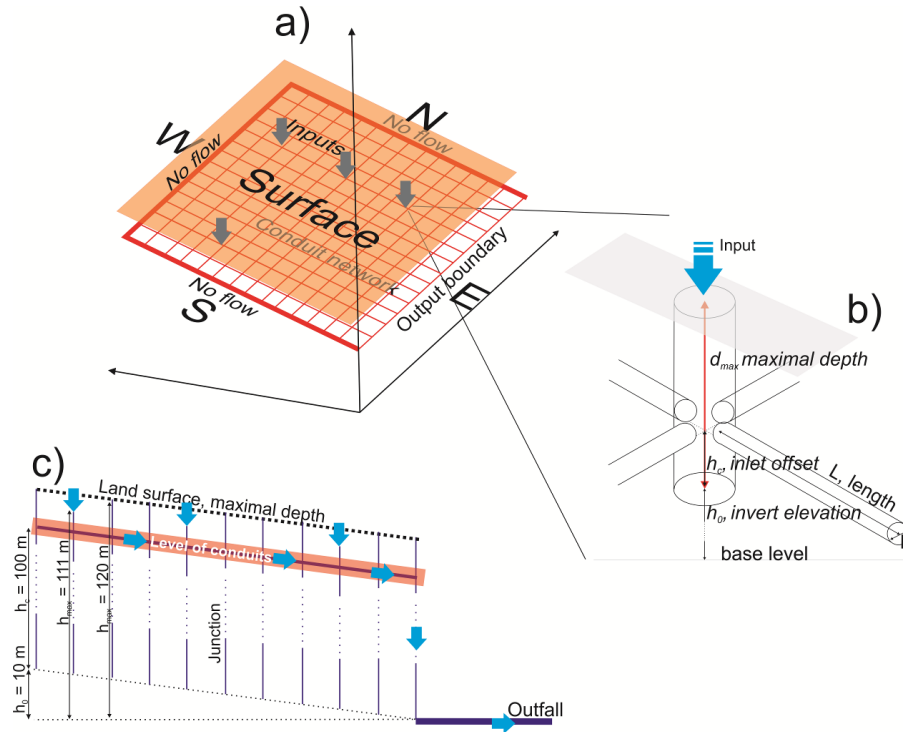


Figure 4. The model structure for the Low dip network. **(a)** A conduit network with discrete water inputs, marked by arrows. Boundaries are denoted geographically. Outputs are along the E boundary. **(b)** Geometry and parameters of a junction. **(c)** The side view of the model, also showing a large conduit connecting E junctions to an outfall.

Evolution of karst conduit networks

M. Perne et al.

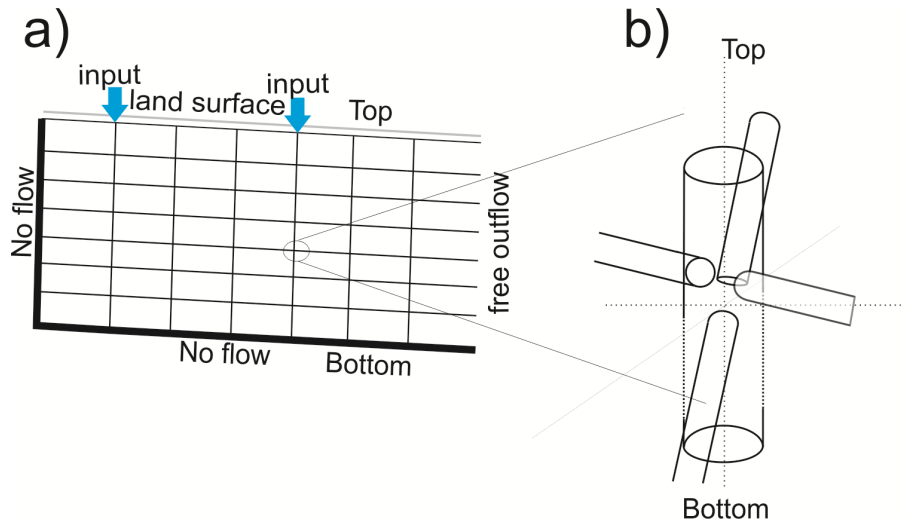


Figure 5. The model structure for the High dip case. **(a)** The slope of the network is 0.99 in from top to bottom and 0.1 m from left to right. The right boundary is a seepage face with free outflow. Inputs are on the top. **(b)** Junction geometry: high dip (“vertical”) conduits are positioned below the low dip (“horizontal”) conduits.

Evolution of karst conduit networks

M. Perne et al.

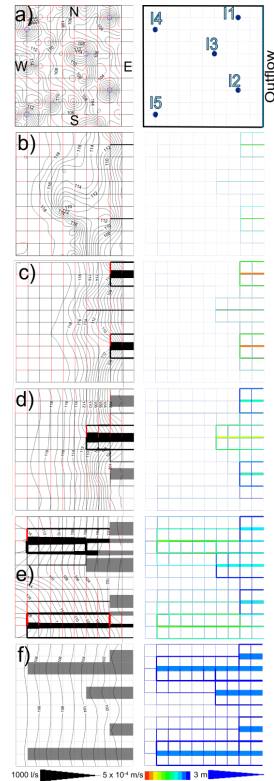


Figure 6. Six snapshots of the evolution of Low-dip network with uniform initial diameters and inlet offsets. Left: flow rates (width) and flow direction (Red = flow towards E or towards N, Black/Grey = flow towards W or towards S). Right: diameters (width) and widening rates (colour). The codes below show thicknesses, flow rates and widening rate. The values at the bar codes correspond to the thickest lines in the flow rate and diameter bars and to the warmest colour in the bar for the widening rate. The scales are linear with the thinnest lines and dark blue colours representing no flow, no widening the and smallest initial diameter.

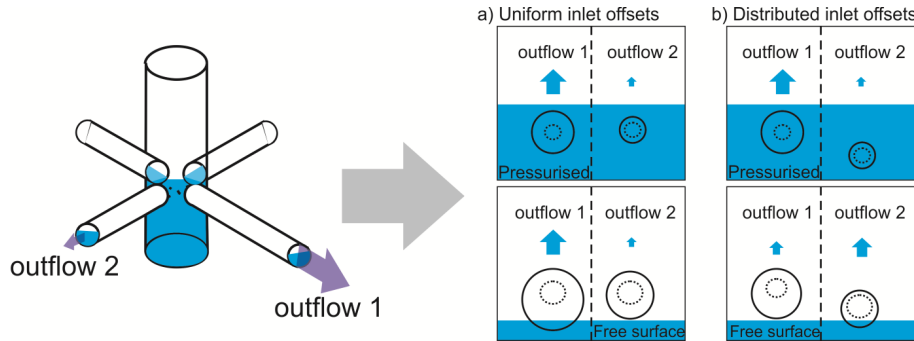


Figure 7. Left: the geometry of a junction. Right (a and (b): Scheme of two outflows during pressurised flow (top) and free surface flow (bottom). (a) initial inlet offsets for both outflows are equal. (b) Initial inlet offset of outflow 2 is smaller so that the outflow has a lower elevation. Blue arrows indicate the amount of flow drained by each outflow, and the blue shading indicates the water table.

Title Page

Abstract

Introduction

Conclusions

References

Tables

Figures

◀

▶

◀

▶

Back

Close

Full Screen / Esc

Printer-friendly Version

Interactive Discussion



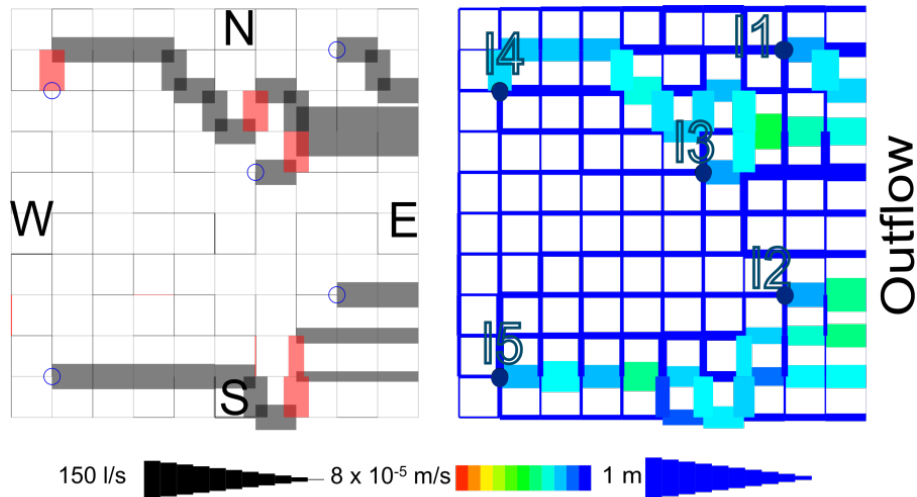


Figure 8. A network with uniform initial diameters and initial inlet offsets randomly distributed within 1 m.

Evolution of karst conduit networks

M. Perne et al.

| | |
|--------------------------|--------------|
| Title Page | |
| Abstract | Introduction |
| Conclusions | References |
| Tables | Figures |
| ◀ | ▶ |
| ◀ | ▶ |
| Back | Close |
| Full Screen / Esc | |
| Printer-friendly Version | |
| Interactive Discussion | |



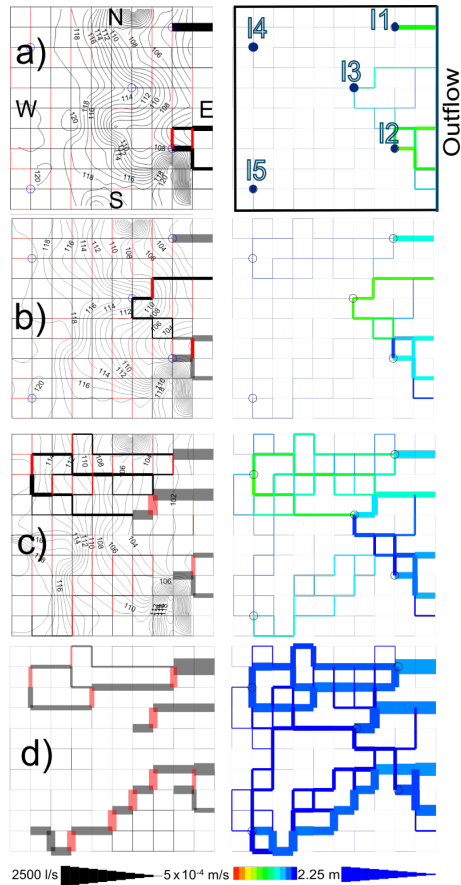


Figure 9. Evolution of a low dip network with randomly distributed initial diameters.

HESSD

11, 6519–6559, 2014

Evolution of karst conduit networks

M. Perne et al.

| | |
|--------------------------|--------------|
| Title Page | |
| Abstract | Introduction |
| Conclusions | References |
| Tables | Figures |
| ◀ | ▶ |
| ◀ | ▶ |
| Back | Close |
| Full Screen / Esc | |
| Printer-friendly Version | |
| Interactive Discussion | |



Evolution of karst conduit networks

M. Perne et al.

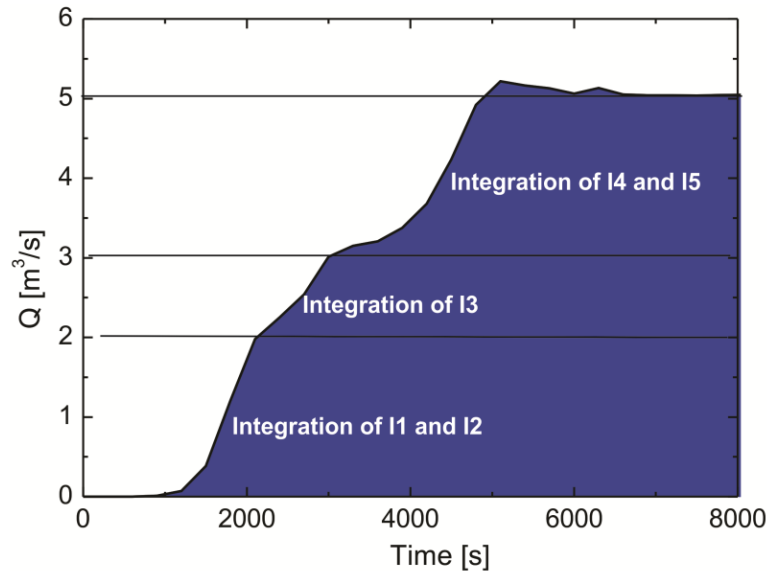


Figure 10. The time evolution of total discharge from the network in Fig. 9.

[Title Page](#)[Abstract](#)[Introduction](#)[Conclusions](#)[References](#)[Tables](#)[Figures](#)[◀](#)[▶](#)[◀](#)[▶](#)[Back](#)[Close](#)[Full Screen / Esc](#)[Printer-friendly Version](#)[Interactive Discussion](#)

Evolution of karst conduit networks

M. Perne et al.

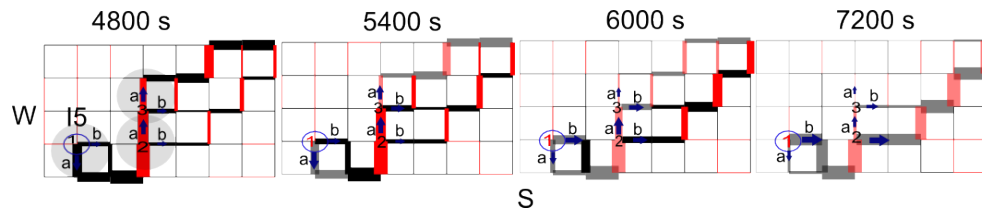


Figure 11. Evolution of SW edge of the network in from Fig. 10 before and after transition to free surface flow.

Title Page

Abstract

Introduction

Conclusions

References

Tables

Figures

◀

▶

◀

▶

Back

Close

Full Screen / Esc

Printer-friendly Version

Interactive Discussion



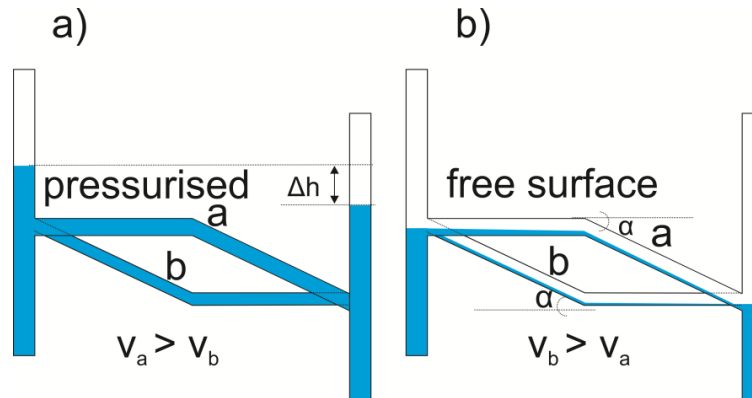


Figure 12. Distribution of flow between two pathways depends on the flow resistance when the flow is pressurised. The pathway (a) has with lower flow resistance grows faster. After the transition to free surface flow, the pathway (b) with higher exit slope from the junction can capture more flow and incise faster.

[Title Page](#)
[Abstract](#)
[Introduction](#)
[Conclusions](#)
[References](#)
[Tables](#)
[Figures](#)
[◀](#)
[▶](#)
[◀](#)
[▶](#)
[Back](#)
[Close](#)
[Full Screen / Esc](#)
[Printer-friendly Version](#)
[Interactive Discussion](#)


Evolution of karst conduit networks

M. Perne et al.

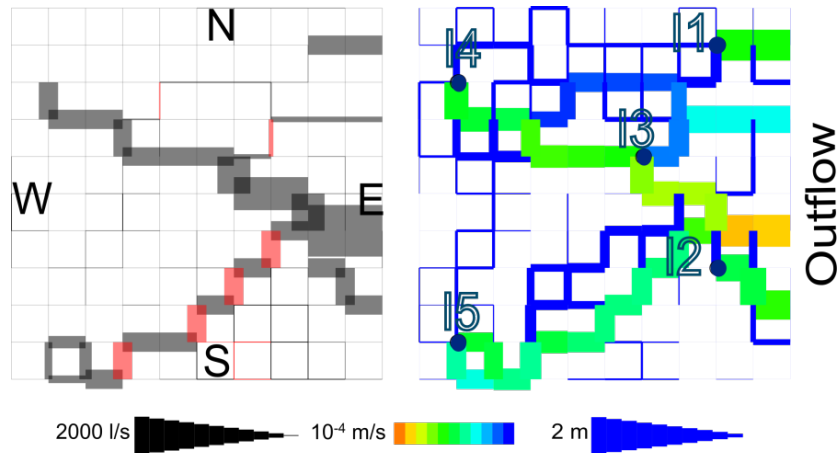


Figure 13. Quasi-stable state of network with same structure as presented in Fig. 9, but the plane of the network is additionally tilted from N to south, for 0.3 m per node.

Title Page

Abstract

Introduction

Conclusions

References

Tables

Figures

◀

▶

◀

▶

Back

Close

Full Screen / Esc

Printer-friendly Version

Interactive Discussion



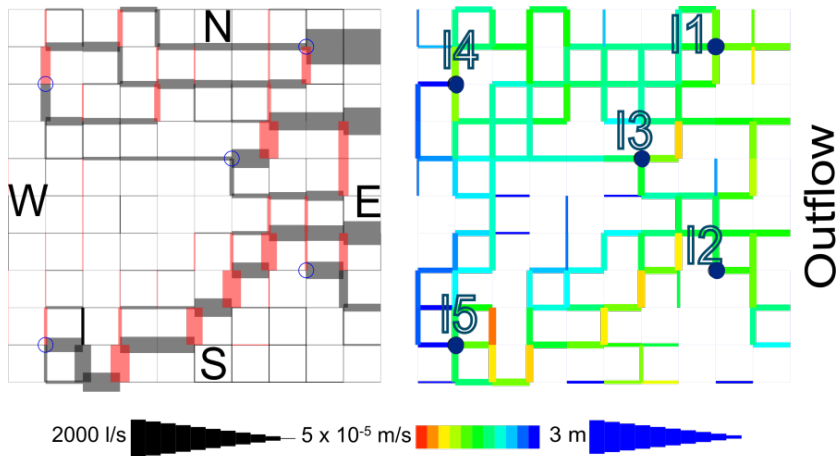


Figure 14. Quasi-stable state for the same scenario as in Fig. 9 with dissolution kinetics for limestone.

Evolution of karst conduit networks

M. Perne et al.

| | |
|--------------------------|--------------|
| Title Page | |
| Abstract | Introduction |
| Conclusions | References |
| Tables | Figures |
| ◀ | ▶ |
| ◀ | ▶ |
| Back | Close |
| Full Screen / Esc | |
| Printer-friendly Version | |
| Interactive Discussion | |



Evolution of karst conduit networks

M. Perne et al.

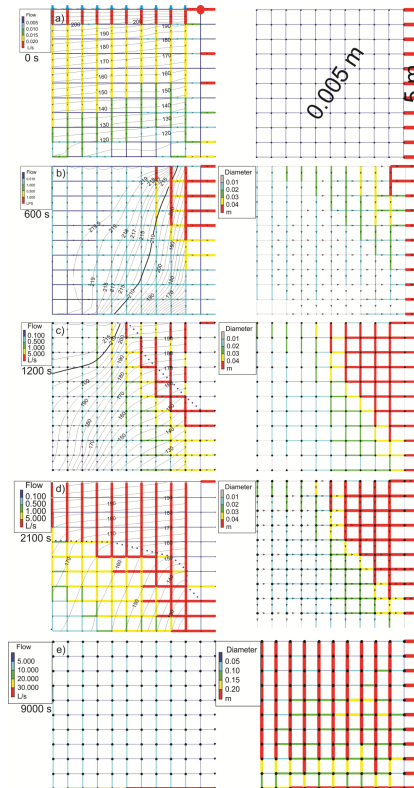


Figure 15. Evolution of homogeneous sub-vertical network. Blue arrows on Fig. 16a denote inputs. Isolines and values present the hydraulic potential [m].

Title Page

Abstract

Introduction

Conclusions

References

Tables

Figures

◀

▶

◀

▶

Back

Close

Full Screen / Esc

Printer-friendly Version

Interactive Discussion



Evolution of karst conduit networks

M. Perne et al.

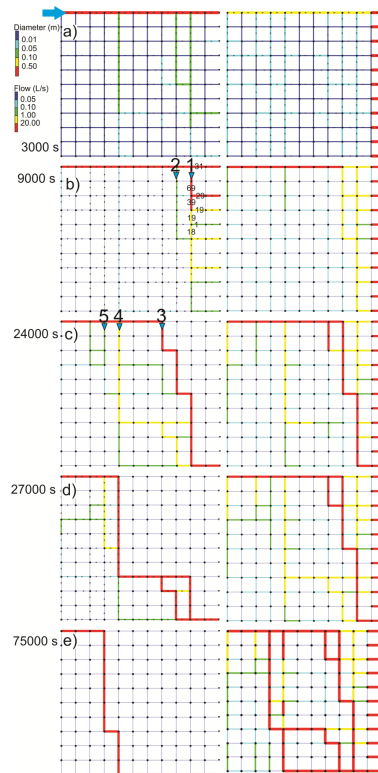


Figure 16. High-dip network with random initial distribution of conduit diameters. Flow enters at the top-left edge of the network as pointed by a blue arrow. Values on (b) show flow rates along the selected individual conduits.

Title Page

Abstract

Introduction

Conclusions

References

Tables

Figures

I◀

▶I

◀

▶

Back

Close

Full Screen / Esc

Printer-friendly Version

Interactive Discussion



Evolution of karst conduit networks

M. Perne et al.

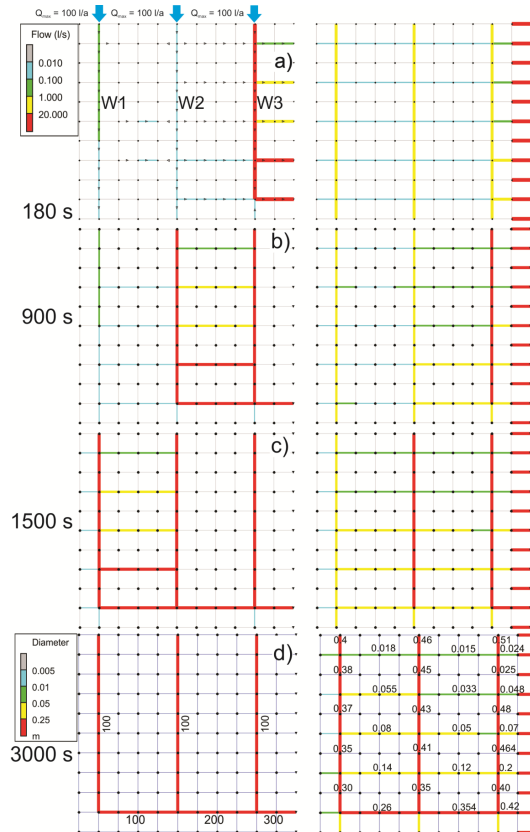


Figure 17. High-dip network with three prominent conduits (wells), marked by W1 to W3. A recharge of 100 L s^{-1} is available to the prominent conduits.

Title Page

Abstract

Introduction

Conclusions

References

Tables

Figures

◀

▶

◀

▶

Back

Close

Full Screen / Esc

Printer-friendly Version

Interactive Discussion

